Bayesian Metric Reconstruction with Gravitational Wave Observations

Sebastian H. Völkel

in collaboration with **Enrico Barausse**

Scuola Internazionale Superiore di Studi Avanzati (**SISSA**), Trieste, Italy
Institute for Fundamental Physics of the Universe (**IFPU**), Trieste, Italy

arXiv:2007.02986 (accepted in Phys. Rev. D)

GReCO seminar

28.09.2020, Institut d'Astrophysique de Paris, France

ERC-2018-COG GRAMS 815673

1 INTRODUCTION

2 METHODS

3 RESULTS

4 DISCUSSION

5 CONCLUSIONS

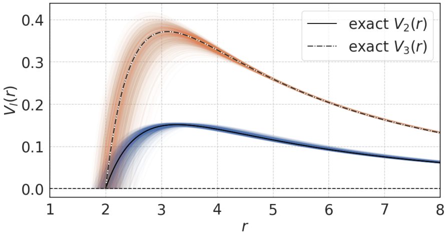

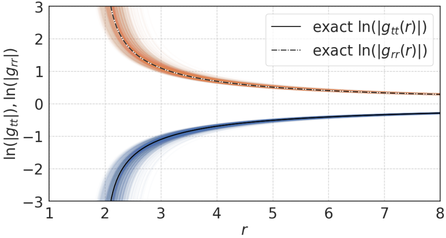

Can one hear the shape of a black hole?

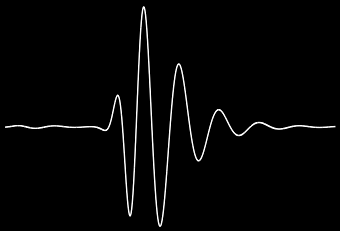

Can one hear the shape of a black hole?

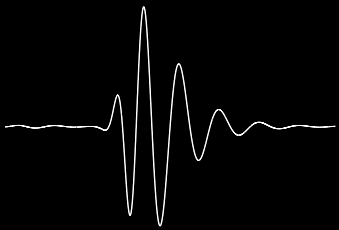

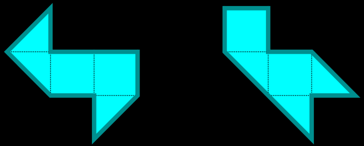

BLACK HOLE RINGDOWN

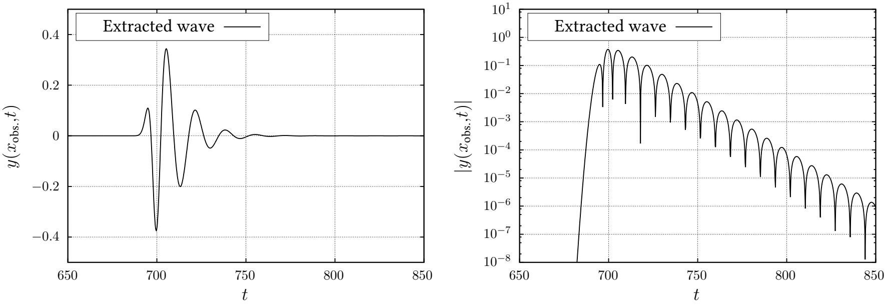

FIGURE 1: Time evolution of a perturbation that scattered with a black hole as seen by an observer far away (left normal scale, right log scale).

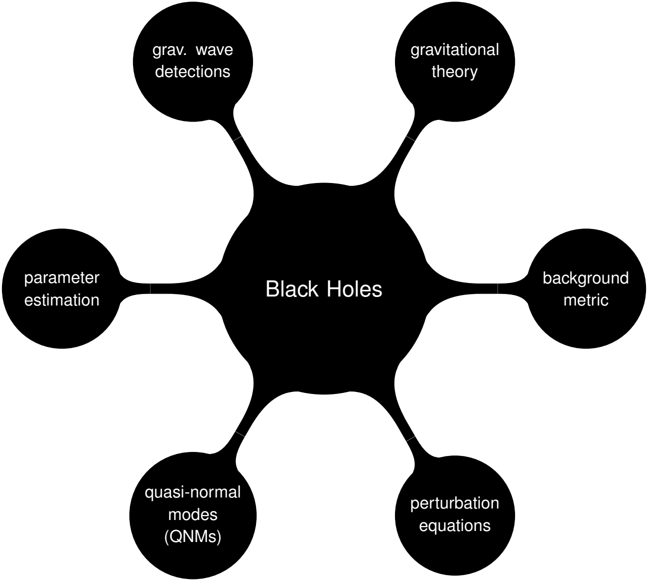
Black Holes
grav. wave detections
gravitational theory
parameter estimation
background metric
quasi-normal modes (QNMs)
perturbation equations

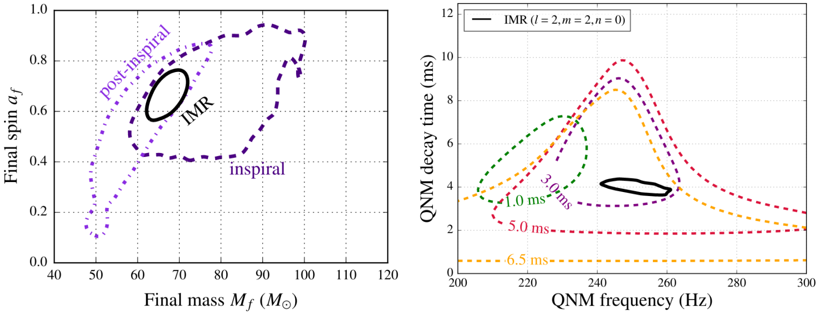

FIGURE 2: **Left:** Reconstructed final mass M_f and final spin a_f using different parts of the signal. **Right:** Reconstructed $l = m = 2$, $n = 0$ QNM frequency and damping time using different starting times as well as IMR result. Taken from B.P. Abbott et al. (LIGO Scientific and Virgo Collaborations), Phys. Rev. Lett. 116, 221101, 2016, `https://doi.org/10.1103/PhysRevLett.116.221101`, [1]

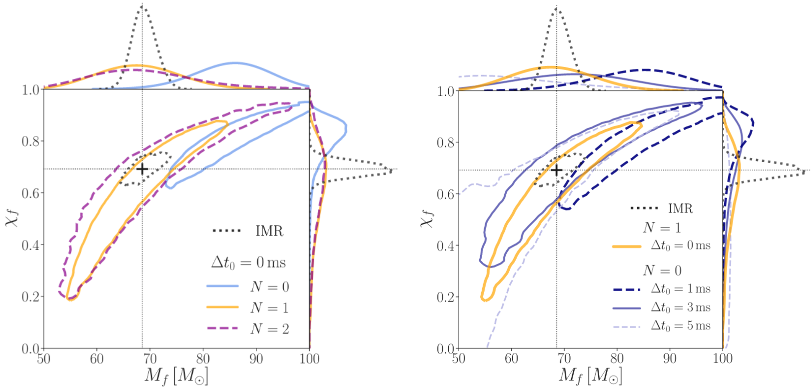

FIGURE 3: Reconstructed final mass M_f and final spin magnitude χ_f. **Left**: using different overtone numbers to fit the ringdown, as well as IMR result. **Right**: as function of different starting times and overtone numbers, as well as IMR. Taken from Maximiliano Isi, Matthew Giesler, Will M. Farr, Mark A. Scheel, and Saul A. Teukolsky, Phys. Rev. Lett. 123, 111102, 2019, https://doi.org/10.1103/PhysRevLett.123.111102, [2]

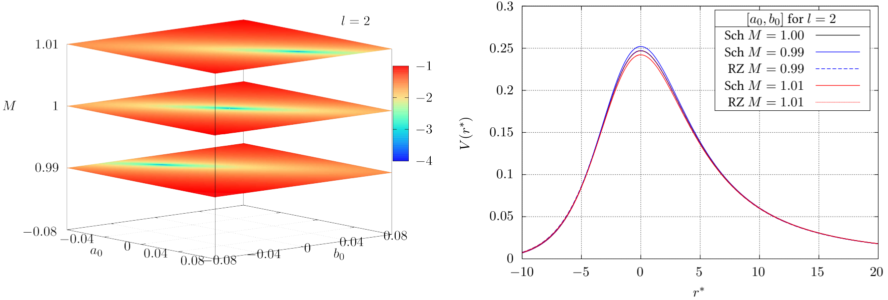

FIGURE 4: **Left:** Combined relative errors of the $l = 2, n = 0$ QNM for different combinations of $\{M, a_0, b_0\}$ and Schwarzschild $M = 1$ as reference. **Right:** Some of the corresponding perturbation potentials. Taken from SHV and Kostas D. Kokkotas, Phys. Rev. D 100, 044026 2019, `https://doi.org/10.1103/PhysRevD.100.044026`, [3].

METHODS OVERVIEW

Our framework has several “building blocks”:

METHODS OVERVIEW

Our framework has several "building blocks":

- parametrized black hole space-time (Rezzolla-Zhidenko metric)
- perturbation equations ($\delta R_{\mu\nu} = 0$)
- computation of QNMs (higher order WKB method)
- RZ models, QNM subsets, QNM precision
- Bayesian analysis via Markov chain Monte Carlo (PYMC3)

METHODS OVERVIEW

Our framework has several “building blocks”:

- parametrized black hole space-time (Rezzolla-Zhidenko metric)
- perturbation equations ($\delta R_{\mu\nu} = 0$)
- computation of QNMs (higher order WKB method)
- RZ models, QNM subsets, QNM precision
- Bayesian analysis via Markov chain Monte Carlo (PYMC3)

Blocks can be modified, general idea is the same!

BACKGROUND METRIC

We use the Rezzolla-Zhidenko (RZ) metric[1]

- parametrization for spherically symmetric and static black holes
- continued fraction expansion for $\tilde{A}(x)$ and $\tilde{B}(x)$
- relation to PPN parameters β and γ possible

$$\mathrm{d}s^2 = -N^2(r)\mathrm{d}t^2 + \frac{B^2(r)}{N^2(r)}\mathrm{d}r^2 + r^2\mathrm{d}\Omega^2, \qquad x \equiv 1 - \frac{r_0}{r}, \qquad N^2 = xA(x), \tag{1}$$

[1] Rezzolla and Zhidenko [4], Phys. Rev. D 90, 084009, 2014

BACKGROUND METRIC

We use the Rezzolla-Zhidenko (RZ) metric[1]

- parametrization for spherically symmetric and static black holes
- continued fraction expansion for $\tilde{A}(x)$ and $\tilde{B}(x)$
- relation to PPN parameters β and γ possible

$$\mathrm{d}s^2 = -N^2(r)\mathrm{d}t^2 + \frac{B^2(r)}{N^2(r)}\mathrm{d}r^2 + r^2\mathrm{d}\Omega^2, \qquad x \equiv 1 - \frac{r_0}{r}, \qquad N^2 = xA(x), \tag{1}$$

$$A(x) = 1 - \varepsilon(1-x) + (a_0 - \varepsilon)(1-x)^2 + \tilde{A}(x)(1-x)^3, \tag{2}$$

$$B(x) = 1 + b_0(1-x) + \tilde{B}(x)(1-x)^2. \tag{3}$$

[1] Rezzolla and Zhidenko [4], Phys. Rev. D 90, 084009, 2014

BACKGROUND METRIC

We use the Rezzolla-Zhidenko (RZ) metric[1]

- parametrization for spherically symmetric and static black holes
- continued fraction expansion for $\tilde{A}(x)$ and $\tilde{B}(x)$
- relation to PPN parameters β and γ possible

$$\mathrm{d}s^2 = -N^2(r)\mathrm{d}t^2 + \frac{B^2(r)}{N^2(r)}\mathrm{d}r^2 + r^2\mathrm{d}\Omega^2, \qquad x \equiv 1 - \frac{r_0}{r}, \qquad N^2 = xA(x), \tag{1}$$

$$A(x) = 1 - \varepsilon(1-x) + (a_0 - \varepsilon)(1-x)^2 + \tilde{A}(x)(1-x)^3, \tag{2}$$

$$B(x) = 1 + b_0(1-x) + \tilde{B}(x)(1-x)^2. \tag{3}$$

$$\varepsilon = -\left(1 - \frac{2M}{r_0}\right), \qquad a_0 = \frac{(\beta-\gamma)(1+\varepsilon)^2}{2}, \qquad b_0 = \frac{(\gamma-1)(1+\varepsilon)}{2}. \tag{4}$$

[1] Rezzolla and Zhidenko [4], Phys. Rev. D 90, 084009, 2014

PERTURBATION EQUATIONS

We study "theory agnostic" gravitational axial perturbations

- we consider $\delta R_{\mu\nu} = 0$ for the RZ metric
- corresponds to GR, but also holds for some scalar tensor theories

$$\frac{\mathrm{d}^2}{\mathrm{d}r^{*2}} Z + \left[\omega^2 - V_l(r)\right] Z = 0\,, \tag{5}$$

PERTURBATION EQUATIONS

We study "theory agnostic" gravitational axial perturbations

- we consider $\delta R_{\mu\nu} = 0$ for the RZ metric
- corresponds to GR, but also holds for some scalar tensor theories

$$\frac{\mathrm{d}^2}{\mathrm{d}r^{*2}} Z + \left[\omega^2 - V_l(r)\right] Z = 0\,, \tag{5}$$

- also include parametrized modification of the potential (K)

$$V_l(r) = \frac{l(l+1)}{r^2} N^2(r) - \frac{K}{r} \frac{\mathrm{d}}{\mathrm{d}r^*} \frac{N^2(r)}{B(r)}\,, \tag{6}$$

QUASI-NORMAL MODES / WKB

Quasi-Normal Modes (QNMs) describe ringdown of black holes

- defined by purely outgoing ($r \to \infty$) and ingoing ($r \to r_0$) waves
- computation of QNMs via higher order WKB method

$$\frac{iQ_0}{\sqrt{2Q_0''}} - \Lambda_2 - \Lambda_3 - \Lambda_4 - \Lambda_5 - \Lambda_6 = n + \frac{1}{2}, \tag{7}$$

with $Q(r^*) \equiv \omega_n^2 - V_l(r^*)$ evaluated at the maximum of potential[2].

[2] R. A. Konoplya, Phys. Rev. D 68, 024018, 2003, [5]

QUASI-NORMAL MODES / WKB

Quasi-Normal Modes (QNMs) describe ringdown of black holes

- defined by purely outgoing ($r \to \infty$) and ingoing ($r \to r_0$) waves
- computation of QNMs via higher order WKB method

$$\frac{iQ_0}{\sqrt{2Q_0''}} - \Lambda_2 - \Lambda_3 - \Lambda_4 - \Lambda_5 - \Lambda_6 = n + \frac{1}{2}, \qquad (7)$$

with $Q(r^*) \equiv \omega_n^2 - V_l(r^*)$ evaluated at the maximum of potential[2].

$$\Lambda_2(n) = \Big((-11(V^{(3)})^2 + 9V^{(2)}V^{(4)} - (30(V^{(3)})^2)n + \qquad (8)$$

$$18V^{(2)}V^{(4)}n - (30(V^{(3)})^2)n^2 + 18V^{(2)}V^{(4)}n^2)\Big)/144(V^{(2)})^2 \qquad (9)$$

[2] R. A. Konoplya, Phys. Rev. D 68, 024018, 2003, [5]

RZ MODELS AND QNM SPECTRA

Choose finite number of RZ parameters and available QNMs

RZ models

- $\text{model}_1 \equiv \{M, \varepsilon\}$
- $\text{model}_2 \equiv \{M, \varepsilon, a_0, b_0\}$
- $\text{model}_3 \equiv \{M, \varepsilon, a_1, b_1\}$
- $\text{model}_{K1} \equiv \{M, \varepsilon, K\}$
- $\text{model}_{K2} \equiv \{M, \varepsilon, a_0, b_0, K\}$

RZ MODELS AND QNM SPECTRA

Choose finite number of RZ parameters and available QNMs

RZ models

- model$_1 \equiv \{M, \varepsilon\}$
- model$_2 \equiv \{M, \varepsilon, a_0, b_0\}$
- model$_3 \equiv \{M, \varepsilon, a_1, b_1\}$
- model$_{K1} \equiv \{M, \varepsilon, K\}$
- model$_{K2} \equiv \{M, \varepsilon, a_0, b_0, K\}$

QNM spectra

- spectrum$_1 \equiv \{l = 2, n = [0, 1]\}$
- spectrum$_2 \equiv \{l = [2, 3], n = [0, 1]\}$

RZ MODELS AND QNM SPECTRA

Choose finite number of RZ parameters and available QNMs

RZ models

- model$_1 \equiv \{M,\, \varepsilon\}$
- model$_2 \equiv \{M,\, \varepsilon,\, a_0,\, b_0\}$
- model$_3 \equiv \{M,\, \varepsilon,\, a_1,\, b_1\}$
- model$_{K1} \equiv \{M,\, \varepsilon,\, K\}$
- model$_{K2} \equiv \{M,\, \varepsilon,\, a_0,\, b_0,\, K\}$

QNM spectra

- spectrum$_1 \equiv \{l = 2,\, n = [0,\, 1]\}$
- spectrum$_2 \equiv \{l = [2,\, 3],\, n = [0,\, 1]\}$

We also consider two different precision for both spectra

- relative errors for real and imaginary part of $\pm 10\,\%$ or $\pm 1\,\%$.

BAYESIAN ANALYSIS

Bayes theorem:

$$P(\theta|D) = \frac{P(D|\theta)P(\theta)}{P(D)} \tag{10}$$

with

- θ **parameters of a model**
- D **observed data**

BAYESIAN ANALYSIS

Bayes theorem:

$$P(\theta|D) = \frac{P(D|\theta)\,P(\theta)}{P(D)} \tag{10}$$

with

- θ **parameters of a model**
- D **observed data**

and

- **posterior** $P(\theta|D)$: probability of parameters given the data
- **likelihood** $P(D|\theta)$: probability of data given the parameters
- **prior** $P(\theta)$: probability of parameters before looking at data
- **evidence** $P(D)$: probability of Data

MARKOV CHAIN MONTE CARLO

Markov chain Monte Carlo (MCMC) are a class of algorithms

- directly sample from the posterior distribution
- computationally expensive and details complicated
- many toolkits available, pure application can be easy

MARKOV CHAIN MONTE CARLO

Markov chain Monte Carlo (MCMC) are a class of algorithms

- directly sample from the posterior distribution
- computationally expensive and details complicated
- many toolkits available, pure application can be easy

We use Python based framework PYMC3

- combine it with external C++ code
- use standard Metropolis Hastings algorithm

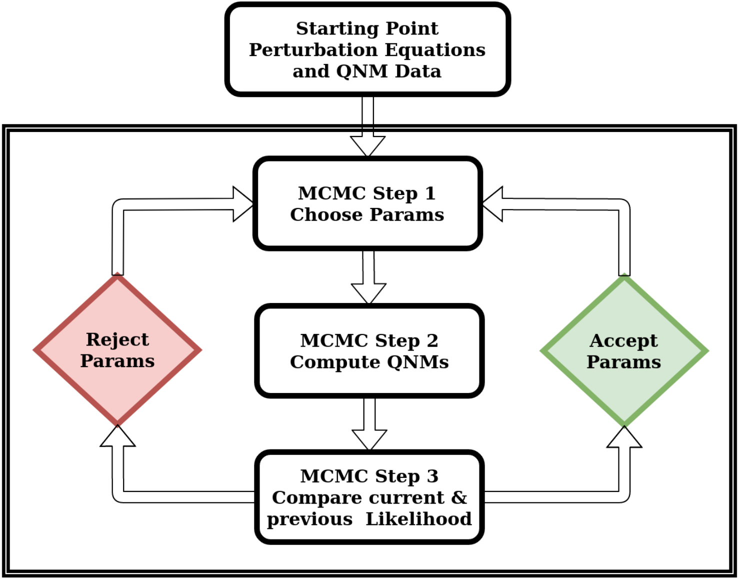
Starting Point
Perturbation Equations
and QNM Data
MCMC Step 1
Choose Params
Reject
Params
MCMC Step 2
Compute QNMs
Accept
Params
MCMC Step 3
Compare current &
previous Likelihood

RESULTS

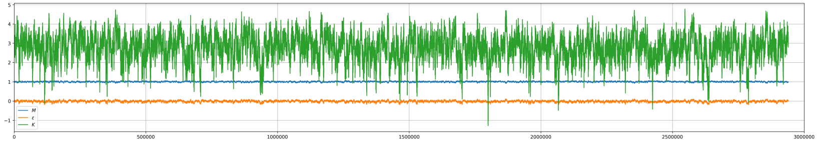
5
4
3
2
1
0
−1
M
ε
K
0
500000
1000000
1500000
2000000
2500000
3000000

Model$_1$ with spectrum$_1$ at $1\,\%$

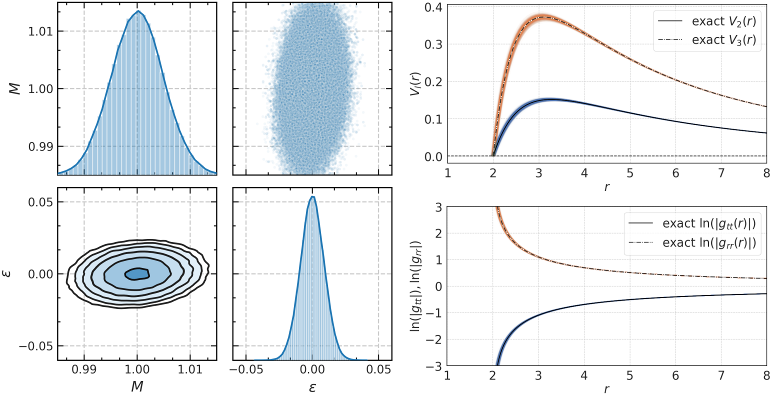

Results for model$_1$ obtained by using spectrum$_1$ with $\pm 1\,\%$ relative error. Left: MCMC parameter estimation. Right top: Exact (black lines) and reconstructed (color lines) potentials $V_2(r)$ and $V_3(r)$. Right bottom: Exact (black lines) and reconstructed (color lines) metric functions $g_{tt}(r)$ and $g_{rr}(r)$.

MODEL$_2$ WITH SPECTRUM$_2$ AT 1 %

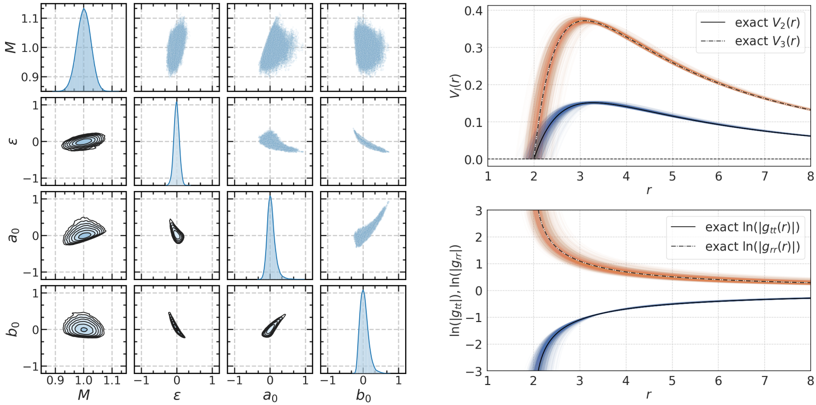

FIGURE 5: Results for model$_2$ obtained by using spectrum$_2$ with $\pm 1\,\%$ relative error. Left: MCMC parameter estimation. Right top: Exact (black lines) and reconstructed (color lines) potentials $V_2(r)$ and $V_3(r)$. Right bottom: Exact (black lines) and reconstructed (color lines) metric functions $g_{tt}(r)$ and $g_{rr}(r)$.

MODEL$_3$ WITH SPECTRUM$_2$ AT 1 %

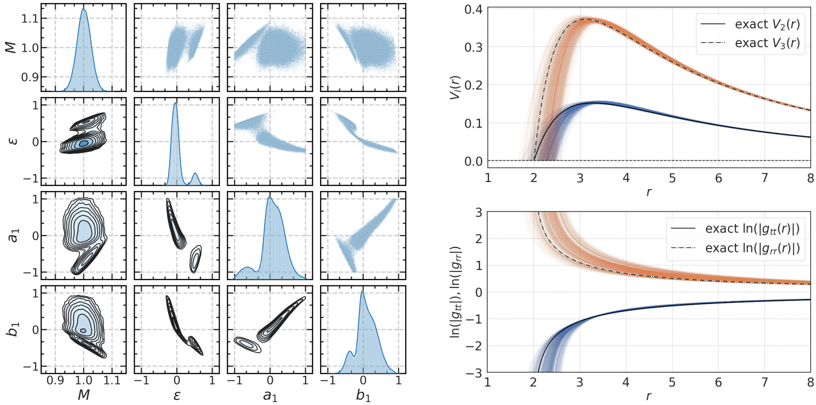

FIGURE 6: Results for model$_3$ obtained by using spectrum$_2$ with $\pm 1\,\%$ relative error. Left: MCMC parameter estimation. Right top: Exact (black lines) and reconstructed (color lines) potentials $V_2(r)$ and $V_3(r)$. Right bottom: Exact (black lines) and reconstructed (color lines) metric functions $g_{tt}(r)$ and $g_{rr}(r)$.

MODEL$_{K1}$ WITH SPECTRUM$_1$ AT $1\,\%$

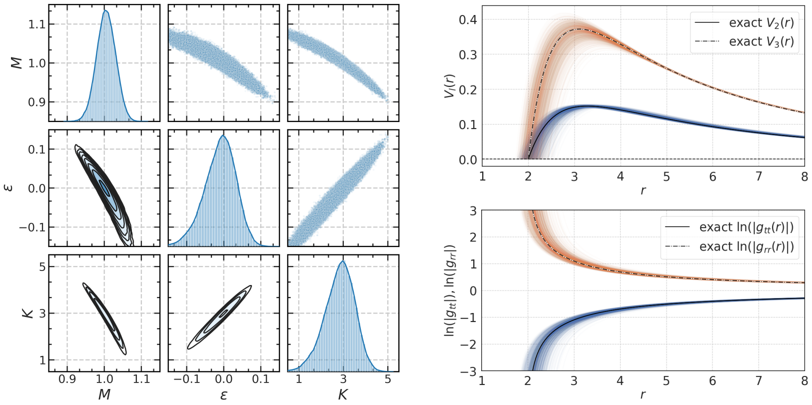

FIGURE 7: Results for model$_{K1}$ obtained by using spectrum$_1$ with $\pm 1\,\%$ relative error. Left: MCMC parameter estimation. Right top: Exact (black lines) and reconstructed (color lines) potentials $V_2(r)$ and $V_3(r)$. Right bottom: Exact (black lines) and reconstructed (color lines) metric functions $g_{tt}(r)$ and $g_{rr}(r)$.

MODEL$_{K2}$ WITH SPECTRUM$_2$ AT $1\,\%$

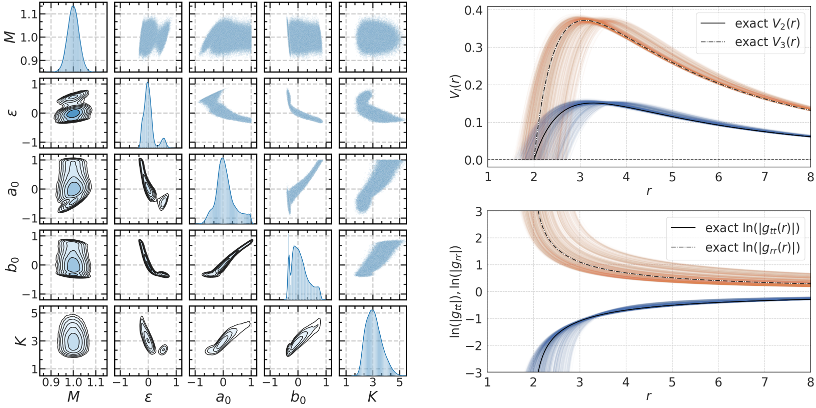

FIGURE 8: Results for model$_{K2}$ obtained by using spectrum$_2$ with $\pm 1\,\%$ relative error. Left: MCMC parameter estimation. Right top: Exact (black lines) and reconstructed (color lines) potentials $V_2(r)$ and $V_3(r)$. Right bottom: Exact (black lines) and reconstructed (color lines) metric functions $g_{tt}(r)$ and $g_{rr}(r)$.

Overall Findings

General observation for models, spectra and precision

OVERALL FINDINGS

General observation for models, spectra and precision

- low dimensional models work well with spectrum$_1$ $(l = 2,\, n = [0,\ 1])$
- higher dimensional models need spectrum$_2$ $(l = [2,\ 3],\, n = [0,\ 1])$
- benefits from $1\,\%$ precise QNMs outperform additional $l = 3$ QNMs
- modified perturbation potential decreases reconstruction mildly
- sampled potentials are suitable for WKB treatment

Relation to Exotic Compact Objects

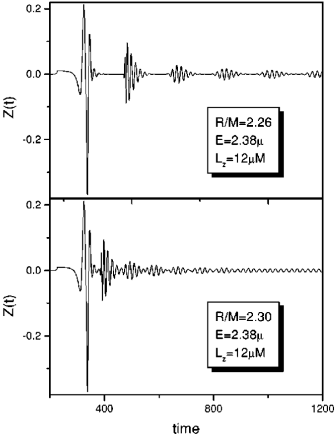

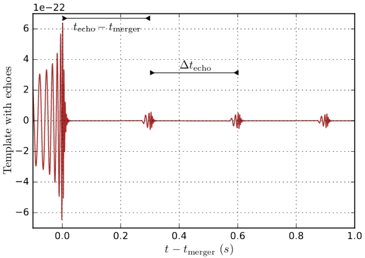

Left: Axial perturbations ultra compact stars, V. Ferrari and K. D. Kokkotas, Phys. Rev. D 62, 107504, 2000.
Right: Echoes from the abyss: Tentative evidence for Planck-scale structure at black hole horizons, Abedi, Dykaar and Afshordi, Phys. Rev. D 96, 082004 2017.

Relation to Exotic Compact Objects

- Inverse problem for horizonless ultra compact objects is different
- **WKB** method and **Bohr-Sommerfeld** rules[3] are powerful here (approximate, but easier to invert)

[3] here $E_n \equiv \omega_n^2$

RELATION TO EXOTIC COMPACT OBJECTS

- Inverse problem for horizonless ultra compact objects is different
- **WKB** method and **Bohr-Sommerfeld** rules[3] are powerful here (approximate, but easier to invert)

$$\int_{x_0}^{x_1} \sqrt{E_n - V(x)}\mathrm{d}x = \pi\left(n + \frac{1}{2}\right) - \frac{i}{4}\exp\left(2i\int_{x_1}^{x_2} \sqrt{E_n - V(x)}\mathrm{d}x\right) \tag{11}$$

[3] here $E_n \equiv \omega_n^2$

INVERTING BOHR-SOMMERFELD RULES

- Known for **single** wells or **single** barriers (**classical BS rule)**[4]
- Extended to **quasi-stationary states** (3 or 4 turning points) [5]
- **Neutron star potentials** with discontinuity (1 turning point) [6]

$$\mathcal{L}_1(E) = x_1 - x_0 = 2\frac{\partial}{\partial E}\int_{E_{\text{min}}}^{E} \frac{n(E') + 1/2}{\sqrt{E - E'}}\mathbf{d}E' \tag{12}$$

$$\mathcal{L}_2(E) = x_2 - x_1 = -\frac{1}{\pi}\int_{E}^{E_{\text{max}}} \frac{(\mathbf{d}T(E')/\mathbf{d}E')}{T(E')\sqrt{E' - E}}\mathbf{d}E' \tag{13}$$

[4] Wheeler [6]; Cole and Good [7]
[5] Völkel and Kokkotas [8]; Völkel [9]; Völkel and Kokkotas [10]
[6] Völkel and Kokkotas [11]

Inverting Bohr-Sommerfeld Rules

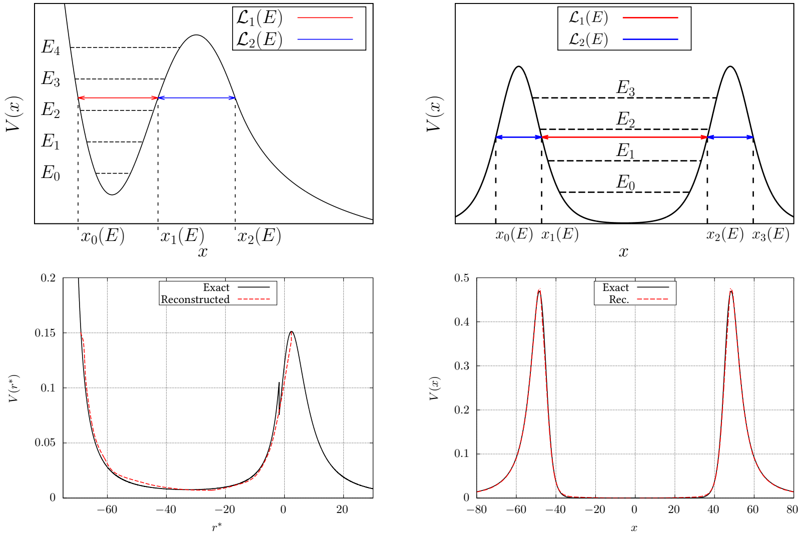

OUTLOOK

Several extensions planned:

- inverse problem for non GR QNMs
- address the rotating case
- combine with other approaches (BH shadows)

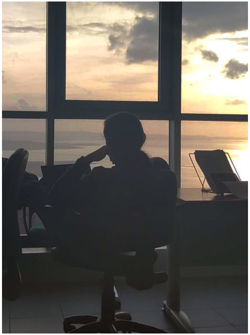

As a proof of principle addressed in this work

As a proof of principle addressed in this work

- Bayesian framework to construct BH metrics from QNMs via MCMC
- allows to quantify constraints on multiple parameters simultaneously
- framework will be extended in multiple directions
- even under idealistic conditions, reconstruction is non-trivial!

As a proof of principle addressed in this work

- Bayesian framework to construct BH metrics from QNMs via MCMC
- allows to quantify constraints on multiple parameters simultaneously
- framework will be extended in multiple directions
- even under idealistic conditions, reconstruction is non-trivial!

Black hole spectroscopy can be used for inverse spectrum problems!

Bibliography I

[1] B. P. Abbott et al. Tests of general relativity with gw150914. *Phys. Rev. Lett.*, 116:221101, May 2016. doi: 10.1103/PhysRevLett.116.221101.

[2] Maximiliano Isi, Matthew Giesler, Will M. Farr, Mark A. Scheel, and Saul A. Teukolsky. Testing the no-hair theorem with GW150914. *Phys. Rev. Lett.*, 123(11):111102, 2019. doi: 10.1103/PhysRevLett.123.111102.

[3] S. H. Völkel and K. D. Kokkotas. Scalar Fields and Parametrized Spherically Symmetric Black Holes: Can one hear the shape of space-time? *Phys. Rev.*, D100(4):044026, 2019. doi: 10.1103/PhysRevD.100.044026.

[4] L. Rezzolla and A. Zhidenko. New parametrization for spherically symmetric black holes in metric theories of gravity. *Phys. Rev. D*, 90:084009, Oct 2014. doi: 10.1103/PhysRevD.90.084009.

[5] R. A. Konoplya. Quasinormal behavior of the D-dimensional Schwarzschild black hole and the higher order WKB approach. *Phys. Rev. D*, 68:024018, Jul 2003. doi: 10.1103/PhysRevD.68.024018.

[6] J. A. Wheeler. *Studies in Mathematical Physics: Essays in Honor of Valentine Bargmann*. Princeton Series in Physics. Princeton University Press, 2015. ISBN 9780608066288.

[7] M. W. Cole and R. H. Good. Determination of the shape of a potential barrier from the tunneling transmission coefficient. *Phys. Rev. A*, 18:1085–1088, Sep 1978. doi: 10.1103/PhysRevA.18.1085.

[8] S. H. Völkel and K. D. Kokkotas. Ultra Compact Stars: Reconstructing the Perturbation Potential. *Class. Quantum Grav.*, 34(17):175015, 2017. doi: 10.1088/1361-6382/aa82de.

BIBLIOGRAPHY II

[9] S. H. Völkel. Inverse spectrum problem for quasi-stationary states. *J. Phys. Commun.*, 2(2): 025029, 2018. doi: 10.1088/2399-6528/aaaee2.

[10] S. H. Völkel and K. D. Kokkotas. Wormhole potentials and throats from quasi-normal modes. *Class. Quantum Grav.*, 35(10):105018, May 2018. doi: 10.1088/1361-6382/aabce6.

[11] S. H. Völkel and K. D. Kokkotas. On the inverse spectrum problem of neutron stars. *Class. Quantum Grav.*, 36(11):115002, Jun 2019. doi: 10.1088/1361-6382/ab186e.

[12] Kazunori Akiyama et al. First M87 Event Horizon Telescope Results. I. The Shadow of the Supermassive Black Hole. *Astrophys. J.*, 875(1):L1, 2019. doi: 10.3847/2041-8213/ab0ec7.

[13] Dimitrios Psaltis et al. *in preparation (2020)*.

$$\tilde{A}(x) = \frac{a_1}{1 + \frac{a_2 x}{1 + \frac{a_3 x}{1 + \dots}}}, \tag{14}$$

$$\tilde{B}(x) = \frac{b_1}{1 + \frac{b_2 x}{1 + \frac{b_3 x}{1 + \dots}}}. \tag{15}$$